Extending the Reach of Anterior Segment Ophthalmic Imaging

by

Shantanu Sinha

Submitted to the Program in Media Arts and Sciences,
School of Architecture and Planning,
in partial fulfillment of the requirements for the degree of

Master of Science in Media Arts and Sciences

at the

MASSACHUSETTS INSTITUTE OF TECHNOLOGY

June 2016

Author ..... Signature redacted

Program in Media Arts and Sciences
May 6, 2016

Certified by ..... Signature redacted

Ramesh Raskar
Associate Professor
Program in Media Arts and Sciences
Thesis Supervisor

Accepted by ..... Signature redacted

Pattie Maes
Academic Head
Program in Media Arts and Sciences

Extending the Reach of Anterior Segment Ophthalmic Imaging

by

Shantanu Sinha

Submitted to the Program in Media Arts and Sciences,
School of Architecture and Planning,
on May 6, 2016, in partial fulfillment of the
requirements for the degree of
Master of Science in Media Arts and Sciences

Abstract

Eye exams via a slit lamp are critical in screening for conditions such as cataracts, corneal opacities and pterygia early on to avert vision loss. The slit lamp, however, is a purely qualitative optical device that is bulky, expensive, can cause eye discomfort due to light sensitivity. It also requires a trained physician to operate, making it unsuitable for large-scale screening in resource-constrained settings. In this thesis, we propose a spectrum of portable anterior segment imaging solutions that can be operated by minimally trained health workers.

On one end, we present a smartphone attachment with minimal optics and no electronic components beyond what is present in the smartphone itself to examine and image the anterior segment of the eye. This cost-effective, easily scalable solution would help extend the reach of anterior segment examination to extremely resource constrained settings, such as mass-screening camps, mobile ophthalmology clinics, war zones etc. On the other end, we propose purely solid-state instrumentation that employs programmable illumination and light steering optics to simulate the motion of a slit on the eye, thereby exhibiting functionality similar to that of a slit lamp with no moving parts. Finally, we discuss potential deployment strategies for two implementations of this technology in the specific cases of two contrasting healthcare systems in India.

Thesis Supervisor: Ramesh Raskar
Title: Associate Professor, Program in Media Arts and Sciences

Extending the Reach of Anterior Segment Ophthalmic Imaging

by

Shantanu Sinha

The following people served as readers for this thesis:

Signature redacted

Thesis Reader .....

Edward Boyden
Associate Professor of Media Arts and Sciences
MIT Program in Media Arts and Sciences

Signature redacted

Thesis Reader .....

Vincent James Patalano II
Assistant Professor of Ophthalmology
Harvard Medical School

Acknowledgements

I would like to thank my advisor, Prof. Ramesh Raskar, for his guidance, support and continual mentorship. His valuable advise and insights have played a crucial role in achieving the results presented in this thesis.

I would like to thank Dr. Vincent James Patalano II for his inputs in formulating the problem statement, clinical mentorship and his help in better defining the potential use cases of the work presented in this thesis. I would like to thank Anshuman Das, Pratik Shah and Guy Satat for their helpful inputs.

Finally, I would like to thank my collaborators at L. V. Prasad Eye Institute and the LVP-MITRA program for their help in building clinic-ready devices and in helping drive device development in the Indian context.

This work was funded by the MIT Tata Center for Technology and Design and the MIT Media Lab consortium.

Results presented in this thesis were captured under the MIT Committee on Animal Care protocol number E15-04-0318 and the MIT Committee on the Use of Humans as Experimental Subjects protocl number 1411006734.

Contents

List of Figures

List of Tables

Chapter 1

Introduction

The human eye is conventionally viewed as having two principal anatomical segments [1]: the anterior segment and the posterior segment. A virtual plane just behind the lens forms the boundary between the two segments. The anterior segment consists of the cornea, iris, lens, ciliary body, and the anterior portion of the sclera. It also includes the anterior chamber, which lies between the cornea and the iris, and the posterior chamber, which lies between the iris and the lens. Both the anterior and posterior chambers are filled with aqueous humor.

A host of disorders [10], such as cataracts, ulcers, pterygia, angle-closure glaucomas etc. affect the anterior segment of the eye and can lead to blindness if left undiagnosed. Specific meaningful clinical interventions are available for each of these common pathologies this form of blindness is completely preventable.

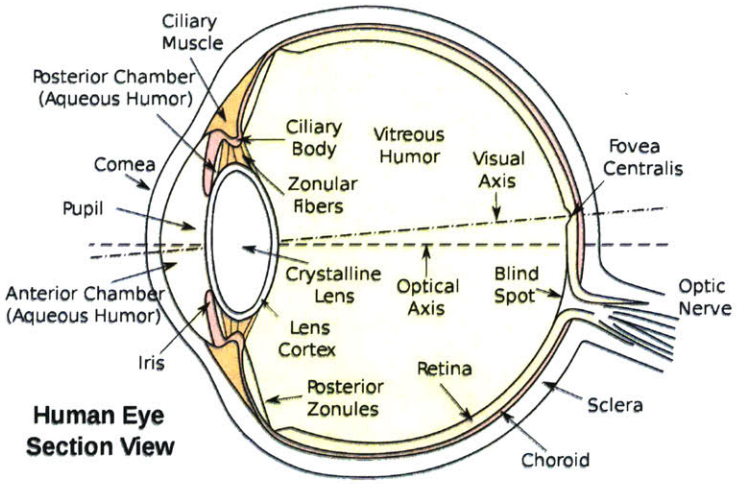

Figure 1-1: Sectional anatomy of the human eye. The lens and all parts of the eye to the left of the lens in the image comprise the anterior segment. (Photo from [4].)

1.1 Motivation

The current standard for screening the anterior segment of the eye is the ophthalmic slit lamp [2]. A slit lamp comprises a high-intensity light source that can be focused to shine a thin sheet of light into the eye. This sheet illuminates a thin slice of the eye, optically isolating it from the rest of the transparent anterior segment. Different layers of the anterior segment have different refractive indices [5], resulting in scattering of light at the boundary of these layers. Thus, from a sufficiently large angle off the optical axis of illumination, a single cross-sectional slice of the anterior segment can be examined. Manipulation of the angle at which this sheet of light hits the surface of the eye allows for viewing different cross-sections of the eye. Various pathologies and conditions affecting the anterior segment manifest themselves as a change in refractive index and scattering properties, which is then picked up by the ophthalmologist.

Though simple in concept, the need for mechanically rotating arms to manipulate the light sheet and eyepiece constrains the form factor and size of the device. A shorter arm length would result in a lower tolerance for error in position of the end of the arm,

Figure 1-2: A conventional benchtop slit lamp. The optics of the device do not make it large - it is ergonomic to have a chin rest and to have the device mounted on a stable platform like a table. In this image the clinician is using an additional handheld lens to examine the retina. (Photo from [3].)

making it harder to illuminate the desired cross-section of the eye. Additionally, the presence of moving parts requires the device to be sufficiently far from the subject's eye to prevent injury.

More advanced techniques such as Scheimpflug imaging [6][7] and OCT [9][8] do exist, but their high cost makes them inaccessible to most, except for the largest ophthalmic clinics and hospitals.

In this thesis we propose a smartphone attachment that utilizes the camera sensor and LED flash of the smartphone for imaging and illumination respectively, thereby providing slit lamp-like imaging without any electronic components over what is present in most commercially available smartphones.

Additionally, we present a new modality to image the anterior segment of the eye using programmable illumination and light steering optics to enable fast, software-driven manipulation of a laser light sheet without any moving parts. We go on to show how this system can be molded into a compact, portable head-mounted device for fully automated data capture in resource constrained settings and discuss the theoretical limitations of such a system.

1.2 Novelty and Primary Contributions

This thesis makes important contributions in showing how consumer electronics can be used to extend the reach of anterior segment examination to resource constrained settings.

- **A smartphone attachment for slit lamp-like imaging of the anterior segment of the eye**

- A 3D printed smartphone attachment with no electronics and minimal optics to produce slit lamp-like images of the anterior segment.
- Use of the LED flash and camera modules present on most commercially available smartphones for illumination and imaging respectively.

- **A programmable illumination-based head mounted device for fast, automated data capture**
  - Use of a commercially available laser pico-projector and light steering optics to simulate the motion of the slit on the eye without any moving parts.
  - Complete programmatic control of the illumination and imaging, enabling the device to be operated by lesser-trained healthcare workers as compared to a conventional slit lamp.

- **Theoretical studies to determine the maximum bounds on performance of a programmable illumination-based device**
  - An ellipsoidal reflector-based optical design that significantly increases the maximum angular sweep of the slit on the eye while producing lower chromatic aberration.
  - Mathematical modeling of the proposed design to explore the dependence of the maximum angular sweep on eccentricity of the ellipse, geometric parameters of the system and throw ratio of the projector.

Chapter 2

Background and Related Work

The conventional slit lamp is used to screen for a wide variety of ophthalmic conditions through illumination of individual cross-sectional slices of the eye separately, thereby enabling the ophthalmologist to mentally reconstruct and inspect the different layers of the anterior segment in great detail, to an extent that is not possible through direct visual examination. The work presented in this thesis aims to present a variety of solutions to extend the reach of slit lamp-like imaging. In this respect, this work draws from three broad areas - ophthalmology, optics and computer graphics. Following are the key developments in each field which form the basis of this work.

2.1 Ophthalmology

Examination of the anterior segment of the eye has not changed considerably for over a century, since the advent of the slit lamp in the early 1900s [11]. One of the earliest designs of the slit lamp was by Alvar Gullstrand in 1911. Gullstrands "large reflection-free ophthalmoscope" employed a Nernst glower as an illumination source

and a simple optical setup to project a slit of light onto the patient's eye. In 1919 Vogt Henker's slit lamp was the first design to mechanically connect the illumination source and the ophthalmoscopic lens [2]. In 1914 Henker proposed a design in which the double articulated arm of the microscope illumination system was not fixed to the table spindle but to the microscope column. This was the first combined connection of microscope and illumination system for co-ordinate motion. Combergs design in 1933 was the first to employ a common swiveling axis for both the illumination and microscopic viewer. In 1938, Haag-Streit engineers proposed a joystick design for x and y coordinate movement [2]. This design was further improved by Littmann in 1950 by employing magnification changers, completing the list of major components of a slit lamp today.

Today, in addition to desktop-mounted slit lamps, smaller, portable slit lamps are also widespread, with most major manufacturers Haag-Streit [12], Keeler [13], Reichert [14] having products in the market. These portable devices operate on the exact same technology as their tabletop counterparts, but are packaged into a smaller form factor. A tabletop slit lamp is not large and bulky because of the size of the individual components, but purely out of ergonomic reasons. It is much easier to use a fixed, desktop-mounted device with a chin rest to lock the subjects face in place and large swiveling arms to achieve small precise rotations. Portable slit lamps are not as ergonomic as their larger counterparts and are, thus, harder to use.

Digital slit lamps can also be found in the market today [15][16][17], but they also operate on the exact same technology, merely replacing the optical eyepiece with a digital sensor. Digital slit lamps whose eyepieces can be replaced with smartphones can also be found [18][19][20]. None of these digital slit lamps apply any major post-processing or extract any additional information from the data captured.

The only known anterior segment imaging modalities that are capable of operating completely automatically, with low to no operator input, are Scheimpflug imaging

[6] and anterior segment optical coherence tomography (OCT) [22]-[25]. The Oculus Pentacam [21] is one such device that operates on the Scheimpflug principle. It employs a mechanically rotating camera and light source to capture different cross-sections of the eye from differnt angles. The slit of light emitted by the device rotates about the axis of the subjects eye, while the camera images the eye off-axis at a fixed position and angle with respect to the source. Tomographic reconstruction techniques are then used stitch these images together to generate a three dimensional (3D) model of the eye [29]. This device is big, bulky and expensive, making it useful for specialized clinics, but not ideal for resource-constrained settings.

2.2 Optical Sectioning

Optical sectioning is a technique well understood in literature to produce cross-sectional views of a 3D refractive object. The objective is to image only those regions of an object that lie either on or close to a defined focal plane and to vastly attenuate or blur light originating from out-of-focus regions of the object.

The simplest way to observe a particular depth is to use a large aperture lens. The large aperture makes the depth of field shallow, and the region outside the depth of field is blurred. Synthetic aperture methods have also been developed to mimic a large virtual aperture by combining many small apertures [26]. However, out of focus depths are still bright and visible, though they are blurred.

Techniques to attenuate light from out of focus depths have been well implemented in microscopy - in confocal microscopy [27] and light sheet fluorescence microscopy [28]. In confocal microscopy contrast of the image is enhanced through the placement of a spatial pinhole at the confocal plane of the lens, thereby blocking light from out of focus depths. In light sheet fluorescence microscopy (LSFM), the problem is addressed differently, through illumination of only the depth that is currently being

imaged. This is achieved using a laser light-sheet which is focused into a single plane, most commonly through the use of a cylindrical lens. This sheet of light can then be moved along the depth of the transparent sample by translating the source along the depth of the sample.

The conventional slit lamp and the Pentacam are both special cases of the application of optical sectioning techniques to ophthalmology. Similar to LSFM, only one cross-section of the eye is illuminated at a time, resulting in no stray light from out-of-focus regions. Unlike LSFM, however, the source of contrast in both these techniques is not fluorescence, but the natural scattering of light at the boundary of different layers of the anterior segment due to changes in refractive index.

2.3 Graphics

Generating accurate 3D models of the eye has been of recent interest to the graphics community. In computer graphics, for a number of years, the shape of the eye was approximated by two spheres one for the cornea and one for the eyeball [31]. In [30], an array of cameras and high-power LEDs are used to generate high-quality 3D models of the eye for animation. This technology, however, requires the subject to be lying down with their head in a headrest under an array of cameras. Additionally, depth is measured through registration of multiple views of the eye from different cameras, not through actual tomography. This results in accurate modeling of the sclera, cornea, iris and pupil, but not of the lens. Also, depth resolution is poor and the model generated is not ideal for medical diagnosis.

There has been recent interest in the computational photography community in the use of commercially available technology for ophthalmic diagnostic applications. This includes smartphone-based screening for refractive errors in [50] and screening for cataracts through measurement of the backscatter produced by the eye lens in [51].

In addition to diagnosis, there have also developments to accomodate for refractive errors in digital displays, such as the light field computational displays in [52][53][54] [69] [71]-[77].

Chapter 3

A Smartphone Attachment for Slit Lamp-like Imaging of the Eye

The slit lamp is the most commonly used ophthalmic device for examining the anterior segment of the eye, but is big, expensive, contains many moving parts and is designed with specialized ophthalmic clinics in mind. In this chapter, we present a smartphone attachment with minimal optics and no electronics beyond the smartphone itself to examine and image the anterior segment of the eye [45]. This cost-effective solution would help extend the reach of anterior segment examination to resource constrained settings well beyond the scope of ophthalmic clinics.

3.1 Concept and Challenges

Most commercially available smartphones today are equipped with high definition cameras and LED flash modules. The flash modules in smartphones serve the purpose of illuminating a scene in poor lighting conditions to capture high quality images.

Unlike flash modules used with standalone cameras, they are rarely capacitor-based light sources and can, hence, be operated continuously. With the right optics to focus the light emitted by the LED into a movable slit and the right camera view, a smartphone attachment could be built for slit lamp-like imaging of the eye without any additional electronics over what is present in the smartphone itself.

There are certain constraints, however, which make building such an attachment challenging -

- **Beam Divergence.** In order to illuminate the entire scene, flash modules are designed to emit light that spreads as wide as possible. This makes it challenging to build a lens system that can collect a large portion of the light to be redirected to the eye in the form of a movable slit.
- **Placement.** Ideally, to reduce the appearance of shadows and to illuminate the scene uniformly, a camera's flash should be co-axial with the camera itself. Practically, however, this is difficult to achieve without affecting image quality and most camera systems, including smartphone cameras, place the flash module as close to the actual imaging sensor as possible, though not co-axial. This makes it challenging to design an attachment that separates the imaging and illumination optical pathways without occluding a significant portion of the camera's view or sacrificing collection of some of the light being emitted by the flash.

3.1.1 Illumination Pathway

In order to capture a significant portion of the light emitted by the flash module we use two high numerical aperture (NA) aspheric condenser lenses to collimate and focus the diverging beam respectively. Aspheric condensers allow larger apertures,

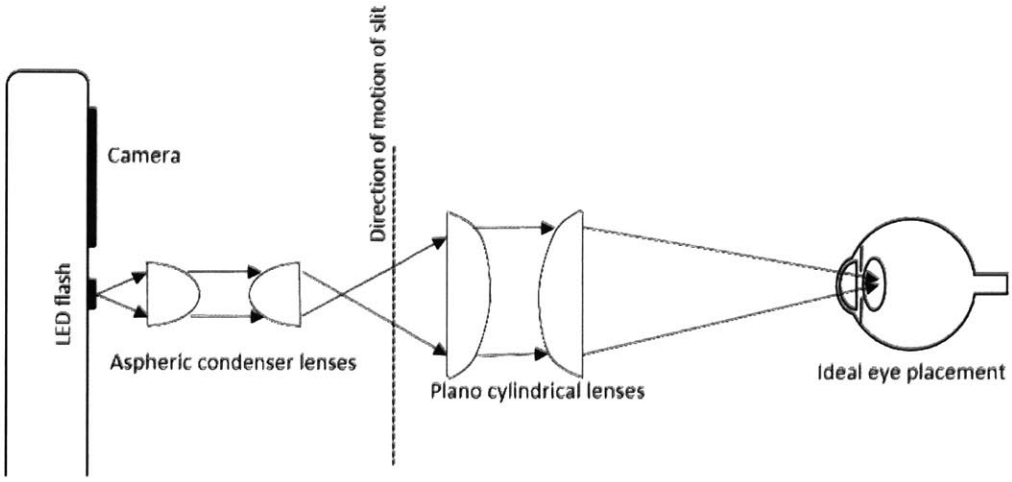

Figure 3-1: Illumination pathway of the smartphone slit lamp attachment: light collection and projection of the image of a slit onto the eye. High NA aspheric condensers are used to collect light from the LED module and low NA cylindrical lenses are used to project an image of the slit onto the eye.

higher NA, and lower f-number ratios than spherical lenses, making them ideal for high-efficiency light gathering. Their short focal lengths and low f-numbers also allow them to be stacked in close proximity to one another, making for a more compact system that can operate within the form factor constraints set by the proximity of the flash module to the imaging sensor.

Following collection by the pair of asheric condensers, we pass the beam through a physical slit that can be moved in a direction orthogonal to the optical axis of the system. The image of this slit is then projected onto the eye through a pair of low NA cylindrical lenses. We intentionally choose large focal length, low NA cylindrical lenses to allow a larger tolerance in the placement of the eye and to ensure that the slit remains in focus on different layers of the eye.

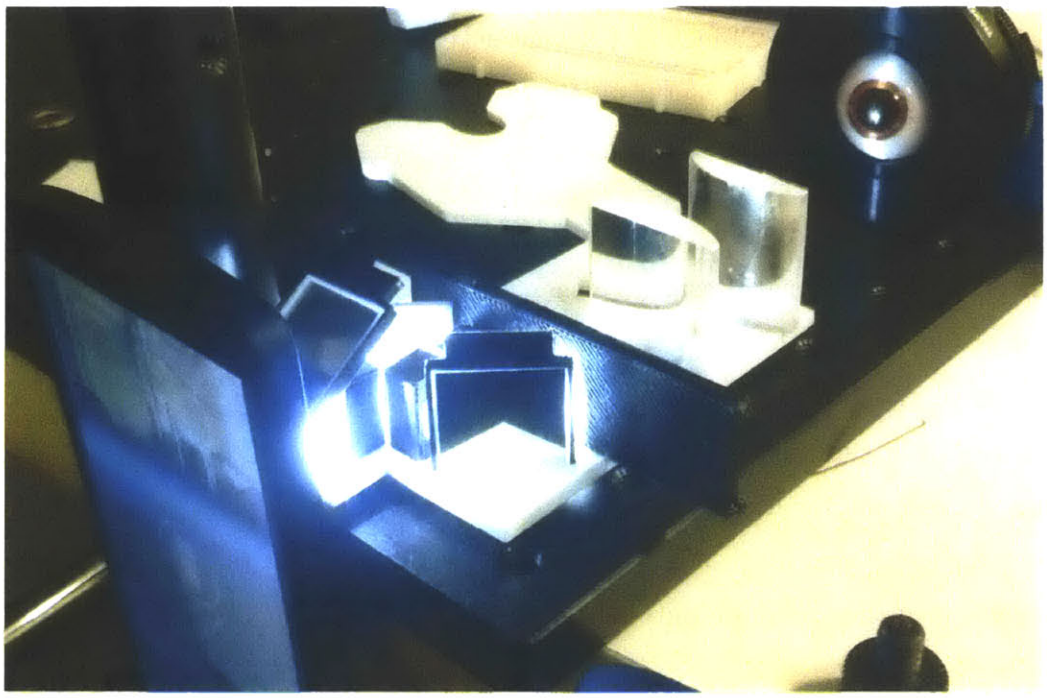

Figure 3-2: Benchtop experimental setup to test optical design presented in section 3.1 on an anatomically correct synthetic eye.

3.1.2 Imaging Pathway

The primary purpose the imaging pathway serves is to change the angle at which the camera "sees" the eye, and to raise the point of view so as to eliminate occlusion of any part of the eye by the illumination optics. As can be seen in 3-1 the camera and LED flash modules in most smartphones are located very close to each other and we must use a pair of first-surface flat mirrors to change the point of view of the camera.

3.2 Experimental Setup

3-2 shows the benchtop setup we built to validate our illumination and imaging optics. We use an off-the-shelf Nexus 5 for this experiment. The Nexus 5 features an 8MP

main camera with a 1/3.2-inch CMOS sensor and an F2.4 30mm equivalent lens. The camera is also capable of capturing 1080p HD video at 30 frames per second. The phone comes with a built-in LED flash that sits 11 mm below the imaging axis.

We use a pair of Edmund Optics 15 mm diameter, 7.3 mm back focal length (12 mm effective focal length) aspheric condenser lenses to collect light from the phone's flash module. These lenses feature a high 0.63 NA, allowing for high efficiency light collection. We use a 3 mm thick acrylonitrile butadiene styrene (ABS) sheet with a 1 mm thick slit, made with a 3D printer. Finally, to focus the image of this slit onto the eye, we use a pair of Thorlabs 38.1 mm focal length plano-cylidrical lenses. The relatively large focal lengths of these lenses allows for a large tolerance in the placement of the eye and ensures that the slit remains focused on different layers of the eyeball.

As can be seen in 3-2, the illumination pathway also comprises two flat mirrors that were not present in 3-1. These mirrors are used to shift the optical axis of illumination slightly to ensure that it is no longer coplanar with the optical axis of imaging. This simply serves the purpose of reducing specular reflection produced by stray light from the flash that escapes the aspheric condenser lenses and can with the images captured by the camera. In an actual smartphone attachment enclosed in a housing, as shown in section 3.3, these mirrors would not be necessary.

The imaging pathway comprises two 20 mm x 20 mm square flat mirrors to change the point of view of the camera. The first mirror is placed directly in front of the camera at an angle of 45^o with respect to the imaging aperture and the second lens is placed at a distance of 5 cm directly above the first at an angle of 60^o with respect to the imaging aperture, as was experimentally found to result in least occlusion and produce the best quality images.

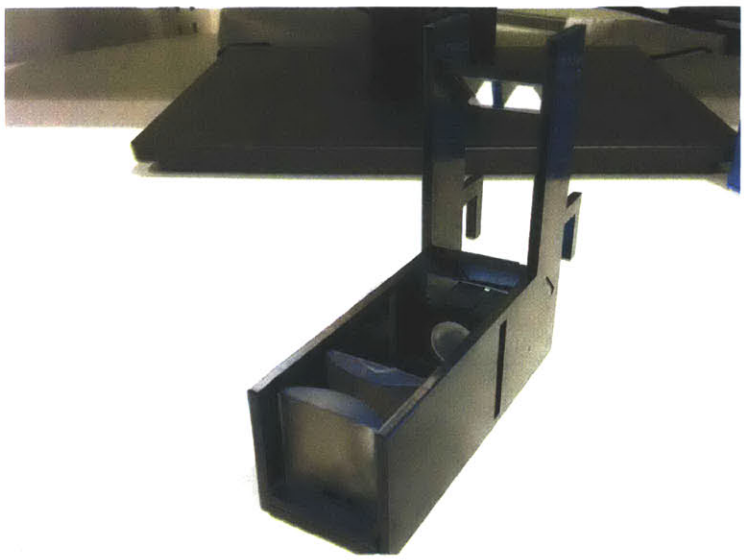

Figure 3-3: A similar optical design to that shown in figure 3-2 is placed inside a housing made of 1/8" thick black acrylic. This image does not show the actual slit, but the slot through which the user moves the slit is visible on the side wall of the device.

3.3 Building a portable device

3-3 shows a prototype smartphone attachment we built, based on the optical design described in 3-1. We built a portable housing around the experimental setup described 3-2 out of 1/8" thick black acrylic. The optical components used in 3-3 are exactly the same as those used in 3-2, except for the absence of the mirrors used in the illumination pathway, which are unnecessary as the housing does not allow stray light from the flash module to affect the images captured by the camera in any way. This housing was designed to fit onto a Nexus 5 smartphone, as shown in 3-4, next to a mannequin head for size comparison.

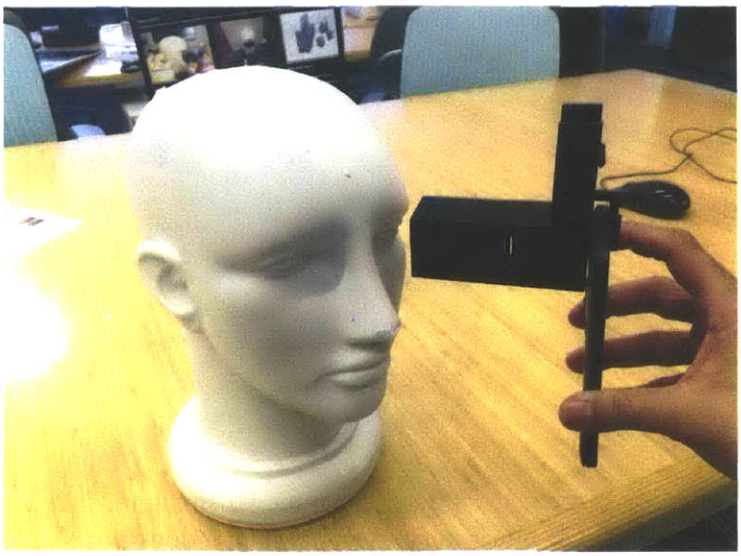

Figure 3-4: The same smartphone attachment as shown in figure 3-3 is shown clipped onto a Nexus 5 smartphone with a mannequin head for size comparison.

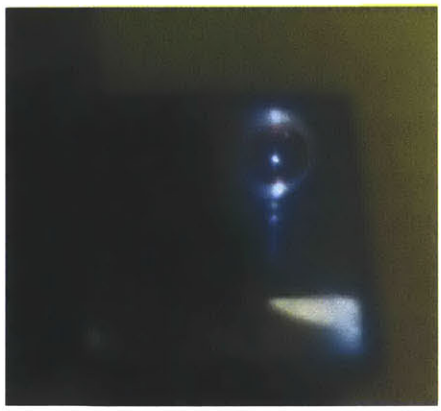

Figure 3-5: Single frame from video sequence captured by the rear camera of the Nexus 5. The slit used was 1 mm thick and was made out of ABS to reduce internal reflections.

3.4 Results and Use-case Studies

The prototype smartphone attachment shown in 3-4 was tested on synthetic anatomically accurate eye models with varying pupil size. 3-5 shows a single frame of a video sequence captured with the rear camera of the Nexus 5 by projecting a slit onto a synthetic eye with a 6 mm pupil. As the slit is mechanically translated along the width of the device, different cross-sections of the eye are illuminated and can be imaged by the built-in camera. Both 3-3 and 3-2 do not show the actual slit, but instead show the slot in the walls of the device through which the user would translate this slit. The slit used in this device was the same as the one used in the benchtop setup shown in 3-2, since ABS is a more diffuse reflector than acrylic and would less in less internal reflection.

Chapter 4

Programmable Illumination-based Imaging of the Eye

The biggest constraint in compressing the optics of a conventional slit lamp is the need for large rotating arms. Shorter arm lengths would result in a lower tolerance for error in position of the end of the arm, making it harder to illuminate the desired cross-section of the eye. Electronic rotation of the arms, say with a stepper motor, would allow much more precise control over the orientation of the light sheet than mechanical movement by an operator, but would still involve moving components that need to be sufficiently away from the eye to prevent injury, resulting in a larger form factor.

In the following sections we describe a new modality for illuminating individual cross-sections of the eye that eliminates the need for moving parts altogether, instead relying on solid-state MEMS components that can be built into a significantly smaller form factor.

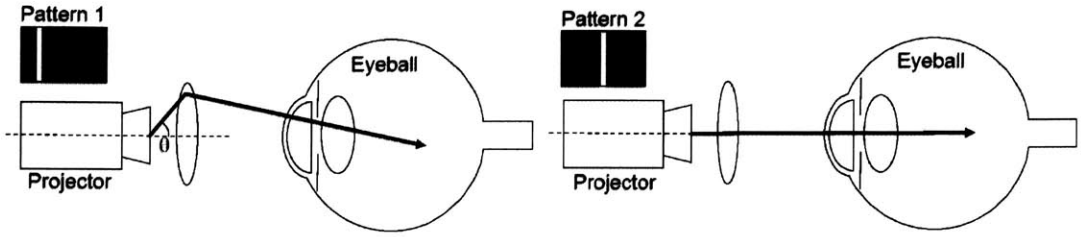

Figure 4-1: Light sheet formation using a laser pico projector. A vertical line is programmatically moved in the frame of the projector, which results in formation of a light sheet that scans the eye, similar to a slit lamp. The high contrast ratio and infinite focus of the laser projector ensure that this light sheet remains sharp at all depths if coupled with the correct light steering optics.

4.1 Illumination

4.1.1 Programmable Illumination

The primary idea proposed in this chapter is to use a MEMS-driven programmable light source, such as a pico projector, to programmatically control the orientation of the light sheet without any moving parts [43]. A conventional, LED-based pico projector requires refocusing of the image based on depth of the screen to produce a sharp image. To avoid refocusing of the illumination, we propose to use a laser pico projector. Unlike an LED projector, each individual pixel in a laser projector is a collimated beam originating from the laser source within the projector. Laser projectors, thus, do not require refocusing for different screen depths.

Laser pico projectors conventionally feature very high contrast ratios, which means the intensity of light projected for dark pixels is many orders of magnitude lower than that for bright pixels. Therefore, if we project a single thin line in the frame of the projector, the resultant beam emitted by the projector very nearly approximates a thin light sheet, with almost no stray illumination from dark pixels. This line can then be moved programmatically in the frame of the projector, to change the orientation

of the sheet of light.

The pico projector can project any computationally generated pattern onto the eye. 4-1 describes how this concept can be extended to produce a moving light sheet, similar to a slit lamp, by projecting a binary line pattern that is translated in software. The width, orientation, direction of motion and scanning speed of this light sheet can be controlled in software to vary the cross-sectional slice of the anterior segment of the eye being illuminated. Additionally, different layers of the eye have different refractive indices, resulting in scattering at the boundary of layers, which serves as a source of contrast in the illumination sectional slice. Most abnormalities in the anterior segment manifest themselves as a change in either the refractive index or scattering properties of the region affected, resulting in high contrast that can be imaged. This method of illumination is, hence, similar to light sheet microscopy, except that the source of scattering is light scatter, not fluorescence.

4.1.2 Light Steering Optics

Projectors are designed to emit diverging beams of light, to produce large images on distant screens. The projected light sheet, would, thus, rotate radially about a virtual spot within the body of the projector. In order to best simulate slit lamp-like illumination it would, hence, be necessary to "steer" this diverging beam, forcing it to converge into a virtual point within the eye being imaged. This would enable examination of cross-sections at a wide range of angles with respect to the optical axis of the system.

4.1.2.1 Single Lens Light Steering

4-2 shows one such simple optical configuration utilizing a single converging lens.

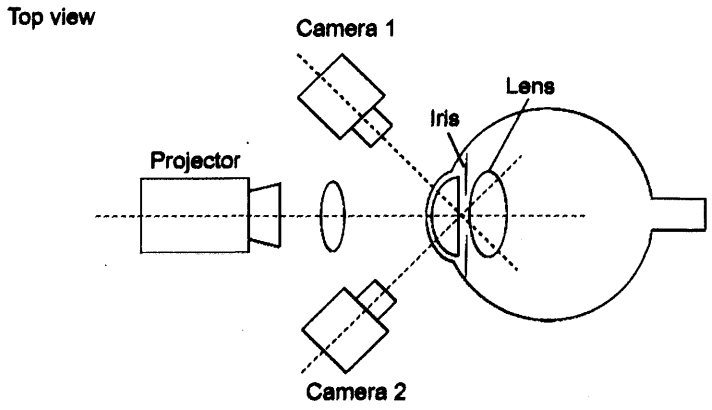

Figure 4-2: A simple optical configuration to steer the beam being emitted by the projector to produce slit lamp-like illumination using a single converging lens. This model suffers from two major drawbacks - the laser projector is no longer able to focus at any depth without an additional focusing lens and the maximum angular sweep possible by the sheet is limited.

This simplistic single lens configuration to steer the light sheet suffers from two major drawbacks

- **Loss of the infinite focusing ability of the laser projector.** The reason laser projectors are able to focus to any screen, irrespective of the distance of the screen from the projector, is because each individual pixel of the projector is, in essence, a collimated beam, similar to a laser pointer. After refraction through the converging lens in this design, however, this will cease to be true, resulting in the projector needing additional focusing optics.

- **Angular sweep range of the slit is limited.** In the proposed single lens design, the angular sweep range of the slit at the eye, β, is a function of the focal length of the lens, f, the diameter of the lens, D, the angle of divergence of the beam emitted by the projector, θ and the distance of the projector from the lens, u. For a given focal length, β would be greatest in the limiting case of the projector being at an infinite distance from the lens, in which case the rays passing through the lens would be parallel, resulting in the beam focusing at a

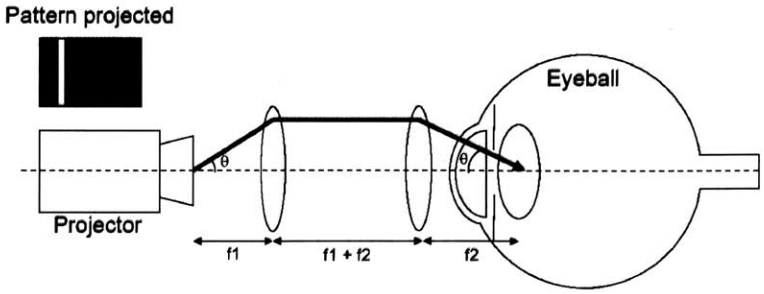

Figure 4-3: An improvement on the design shown in figure 4-2. The first, collimating lens serves the dual purpose of ensuring that laser projector is able to focus at any depth and enabling the second, focusing lens to function in the limiting case of the projector being at infinity with respect to it.

distance f from the lens. In this theoretical limiting case,

$$\beta = 2\tan^{-1}(\frac{D}{2f}) \tag{4.1}$$

This limiting case, however, can never be achieved practically with a single lens as, even at large finite distances, the amount of light emitted by the projector that is collected by the lens will be extremely small, and will be infinitesimally small in the limiting case of $u \to 0$.

In order to address these two issues, we propose a two lens model to steer the beam emitted by the projector.

4.1.2.2 Two Lens Light Steering

4-3 describes the proposed model, comprising two aspheric achromatic converging lenses of focal lengths $f1$ and $f2$. The first lens collimates the beam emitted by the projector and the second lens refocuses it to a virtual point within the eyeball.

By placing the two lenses at a distance of $f1+f2$ apart, we ensure that each collimated pixel emerging from the projector focuses to a point between the two lenses and

remerges as a collimated pixel at the eyeball, thus preserving the infinite focus of the laser projector.

Additionally, since the rays emitted by the projector are collimated by the first lens, the virtual image of the projector is at ∞, even though the projector is at a finite, small distance away and a large portion of the light emitted has been collected by the first lens. In this way, this system behaves like the limiting case of the single lens model described in section 4.1.2.1, and β would be defined by equation 4.1. The sweep angle achieveable with this system is, hence, significantly higher than that possible with a single lens configuration.

4.2 Imaging

The second rotating arm is provided in a slit lamp to allow for adjustments in the viewing direction of the illuminated sectional slice of the eye. 4-4 explains why having a single viewpoint is not ideal to resolve cross-sectional slices of the entire anterior segment. When the light sheet is at the position shown in the figure, the angle between the optical axis of camera 1 and the projected light sheet is α. We call this angle the viewing angle of the slit for camera 1. The image captured by camera 1 is a view of the sectional slice, compressed along one dimension by a factor $\sin\alpha$. For a small α (as in the figure), this compression is significant. Since the data captured by the camera sensor is dicretised, at a small α there is significant information loss in one dimension that cannot be recovered in software. Ideally, we want to view the slice perpendicular to the light sheet at all positions of the sheet to avoid any data loss.

Since the light sheet rotates about a virtual point in the eye, this condition would require the camera to rotate with it. In order to avoid rotation of the camera, we make the approximation of placing cameras at a finite number of viewpoints and use

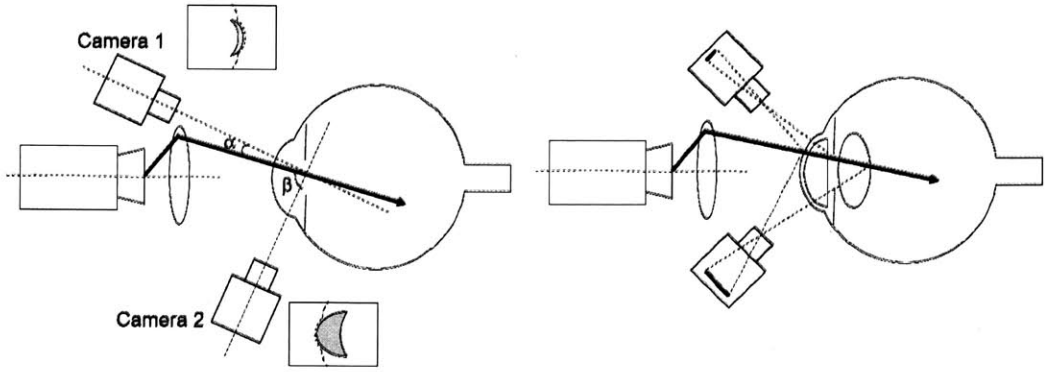

Figure 4-4: Camera 1 has a small viewing angle, α and hence captures an image of the cross-section that is severely compressed along one direction. Camera 2, on the other hand, has a much larger viewing angle, β, close to 90^o and captures an image that can be easily rescaled in software to accurately depict the actual cross-section without significant loss of information.

the image captured by the camera with the highest viewing angle. This image can then be scaled in software by a factor of $(1/\sin\alpha)$, where α is the viewing angle of the camera the image was captured with. If α is large (close to 90^o), loss of resolution would be minimal and the scaled image would preserve significant detail. In 4-4, camera 2, with viewing angle β, would capture much more detail than camera 1. The image captured by camera 2, after scaling by a factor of $(1/\sin\beta)$ would preserve sufficient detail to be a good approximation of the cross-sectional slice being imaged.

For larger viewing angles, however, the margin of error allowed in placement of the eye, ensuring that it stays within the camera view, reduces. As shown in 4-5, projection of a fixation target is able to impose constraints on the placement of the eye in one two dimensions, but the eye is still free to move along the optical axis of the projector.

This means that for a camera placed perfectly on-axis (0^o viewing angle), the margin of error is infinite, since the eye would always be along that axis if the fixation target is in view. For a 90^o viewing angle, however, the margin of error is proportional to the ratio of the field of view of the camera at that depth to the size of the eye (this imposes a lower bound on the margin of error). In general, for any viewing angle, the

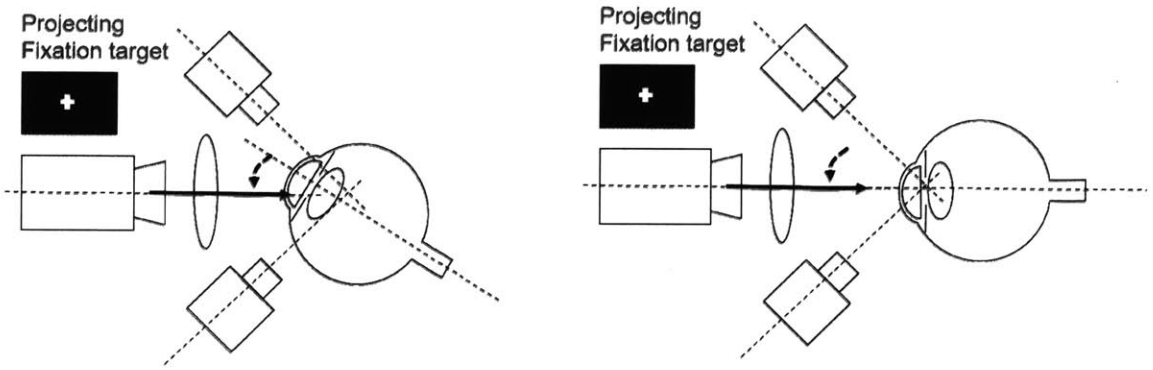

Figure 4-5: Projection of a fixation target helps constrain the position of the eye along all directions but the optical axis. The eye is free to move back and forth on the optical axis and the only change perceived by the subject would be a change in size of the fixation target.

margin of error is proportional to the ratio of the field of view of the camera at that depth to the size of the object scaled by the sine of the viewing angle, meaning larger angles require the eye to be more precisely aligned for the cameras to capture useful data.

In addition to this, the geometry of the eye imposes practical constraints on the range of viewing angles that would result in good data capture. The eye is not purely transparent under visible light illumination - the sclera and the iris are opaque. This would make it impossible to view the lens at a 90^o viewing angle at some slit positions, even if the position of the eye could be precisely controlled, as it would be occluded by the sclera or iris. It becomes necessary to have a small enough viewing angle to be able to image the lens through the pupil, avoiding occlusion by the sclera and the iris..

Experimenting with multiple camera positions, number of viewpoints and eye placements, we determined that having an imaging system comprising two cameras placed at 45^o angles on either side of the optical axis of the illumination is the most practical.

Figure 4-6: Experimental setup of one and two lens models for data capture on bovine, porcine and rabbit eyes *ex vivo*.

4.3 Experimental setup

To experimentally demonstrate this concept, we built a benchtop setup of the two lens model and used it to capture data on bovine, porcine and rabbit eyes *ex vivo*.

- **Illumination.** We used two laser pico projectors in our experiments - the Cellulon PicoPro and the MicroVision PicoP. The Cellulon PicoPro was found to produce a more defined slit. The projector features a 1:3 throw ratio and a contrast ration of 80000:1. The high resolution of the projector allows for 1920 vertical line positions or 720 horizontal line positions, allowing for fine control over the orientation of the light sheet.

- **Light steering optics.** We used two Thorlabs achromatic doublets with a focal length of 30 mm and a diameter of 25.4 mm, coated for operation in the visible range (400-700 nm).

- **Imaging** We used two Point Grey Blackfly color cameras with 1.3 MP sensors to image the eye from two directions. The Blackflys come fitted with global

shutters, preventing corruption of data due to rolling shutter artifacts. Both cameras were placed out of plane of the illumination system at an angle of 45° with respect to the plane of illumination, as shown in 4-6.

- **Software.** We setup the laser projector to project a vertical line of width 8 pixels, experimentally chosen for optimal illumination. The line was translated one line width (8 pixels) at a time, at a refresh rate of 30 Hz, resulting in a total of 160 line positions and a total scan time of just over five seconds. The cameras were synchronized with the projector, to prevent data capture when the laser projector was refreshing to a new slit position. The computer then selected, scaled and stored the image captured with the camera with the highest viewing angle, based on the known position of the light sheet.

4.4 Results

The following figures, show images captured under different conditions on bovine and porcine eyes (MIT Committee on Animal Care protocol number E15-04-0318, MIT Committee on the Use of Humans as Experimental Subjects protocl number 1411006734). 4-12 has not been captured by the authors, but has been shown for comparison purposes. Rabbits have albino irises [47], and the scattering properties of their anterior segments are, hence, quite different from that of humans. The data captured on rabbit eyes was found to be significantly different from that captured on bovine and porcine eyes and is not representative of what can be expected if we were to test this on humans.

Figure 4-7: Image captured with a conventional slit lamp on a human subject (not captured by the authors, for comparison purposes only).

Figure 4-8: Cross-sectional slice of a bovine eye illuminated using two lens model. Image shown was captured with the camera with the larger viewing angle. The thick bluish-white curve is the cornea. The thickness is due to scattering at the boundary of different layers of the cornea. The thin red curve is the iris.

Figure 4-9: The same bovine eye as 4-8, imaged at the same instant with the camera with lower viewing angle. The image was not scaled in software to help illustrate the extent of compression along one dimension due to low viewing angle.

Figure 4-10: Mildly damaged bovine eye, as illuminated by two lens model. Part of the cornea has been scraped off with a scalpel. As can be seen in the figure the central portion of the cornea (thick bluish-white curve) is missing.

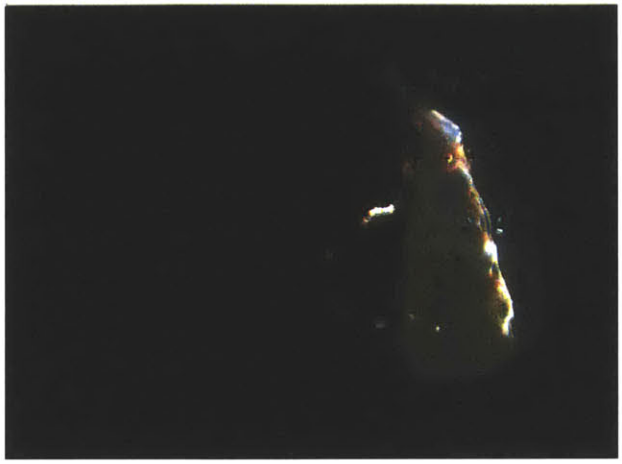

Figure 4-11: Severely damaged bovine eye, as illuminated by two lens model. The cornea and the iris have both been severely damaged with a scalpel. A large amount of scattering is visible due to mixture of different layers of the eye.

Figure 4-12: Cross-sectional slice of a porcine eye illuminated using two lens model. Image shown was captured with the camera with the smaller viewing angle. Once again, the thick bluish-white curve is the cornea and the thin red curve is the iris.

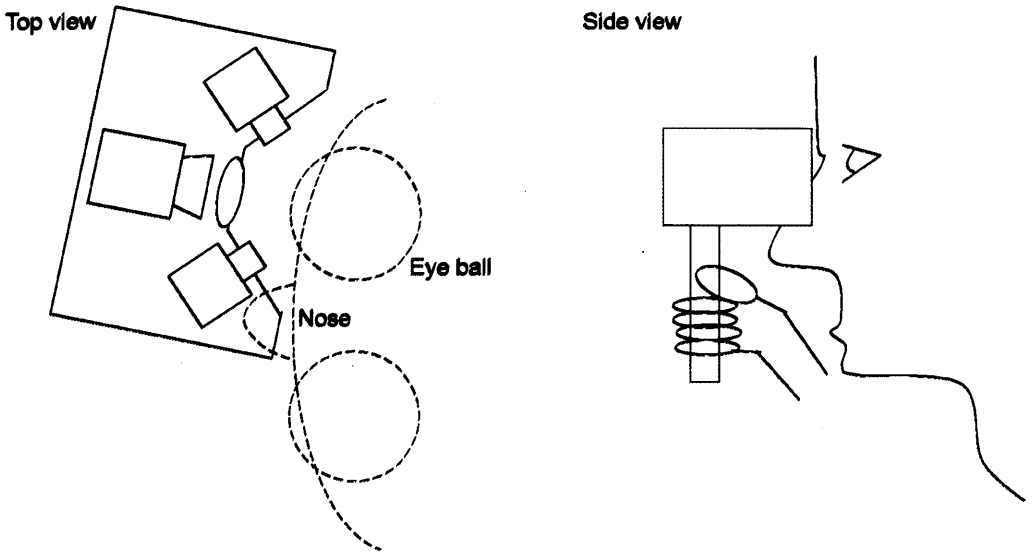

Figure 4-13: A hand-held implementation of the two lens model described in earlier sections would suffer from a number of bad frames due to relative motion between the device and the head. The two lens model described in section 4.3 can capture data on the entire eye in about five seconds, but even at that speed any relative motion would cause significant loss of data.

4.5 Concept Head-mounted prototype

One of the major problems with portable slit lamps is the relative motion between the device and the subject's eyes. Benchtop slit lamps face much less of an issue since the person's head is mounted securely on a chin rest. The solid state device presented in this chapter is capable of capturing data extremely fast (about 5 seconds) compared to a conventional slit lamp, but any head movement would still have a significant effect on the images captured. A portable version of this prototype, such as the hand-held device shown in 4-13, would suffer from significant bad frames due to this relative motion.

In this section we present a concept prototype that attempts to solve this problem by resting directly on the person's head, instead of being in the hands of the operator.

There are two major types of motion that can cause bad data capture by an anterior segment imaging device. We show how this concept device can minimize both.

- **Motion between the subject's head and the device.** Having the device head-mounted eliminates nearly all motion between the head and the device. This is similar to a virtual reality headset, in that the subject wears a device that is strapped onto the back of his or her head and covers both eyes, optically isolating them.

- **Movement of the subject's eyes within his or her head.** This kind of motion is not reduced by simply making the device wearable. The experience provided by a virtual reality headset is not necessarily affected by this kind of motion, but in the case of capturing images of the eyes, this kind of motion can introduce a number of motion blurred or noisy frames. A simple way to restrict motion along directions perpendicular to the optical axis of illumination is by projecting a fixation target that the subject must look at while data is being captured, as shown in 4-5. As was noted earlier, however, a fixation target does not restrict motion along the optical axis of illumination at all. In the case of a head-mounted device, however, as will become clear in 4-14, since the device is designed to be strapped onto the back of the subject's head, this kind of motion is greatly minimized.

4-14 shows a possible implementation of such a device. The device would comprise two sets of illumination and imaging components, with each eye being imaged independent of the other. The projectors could be mounted vertically, as shown in 4-14 and the rays redirected to the eyes using a mirror. This would help center the weight of the device closer to the subject, reducing the torque the subject would feel on his or her neck.

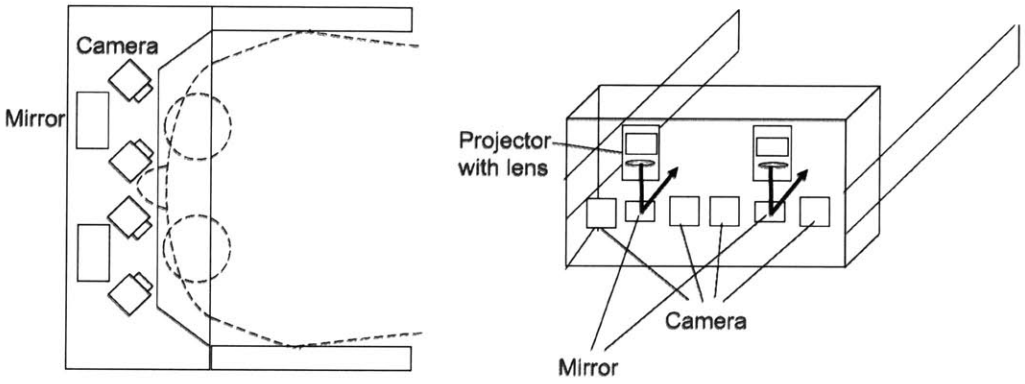

Figure 4-14: Concept head-mounted prototype. Each eye is illuminated and imaged independently and the device is strapped onto the back of the subject's head to reduce relative motion between the device and the subject.

Chapter 5

Theoretical Limits of Programmable Illumination-based Methods

A conventional slit lamp features a angular sweep of close to 180^o. Even with the two lens configuration described, achieving sweep angles in excess of 50^o is impractical, without significant chromatic aberration. In an effort to improve the angular sweep range of the design presented in Chapter 4 to better match that of a conventional mechanical slit lamp, we propose an improved optical design and study the theoretical limits of such a design.

5.1 Proposed concept

The basic purpose of this model is to solve two major problems with the two-lens model described earlier -

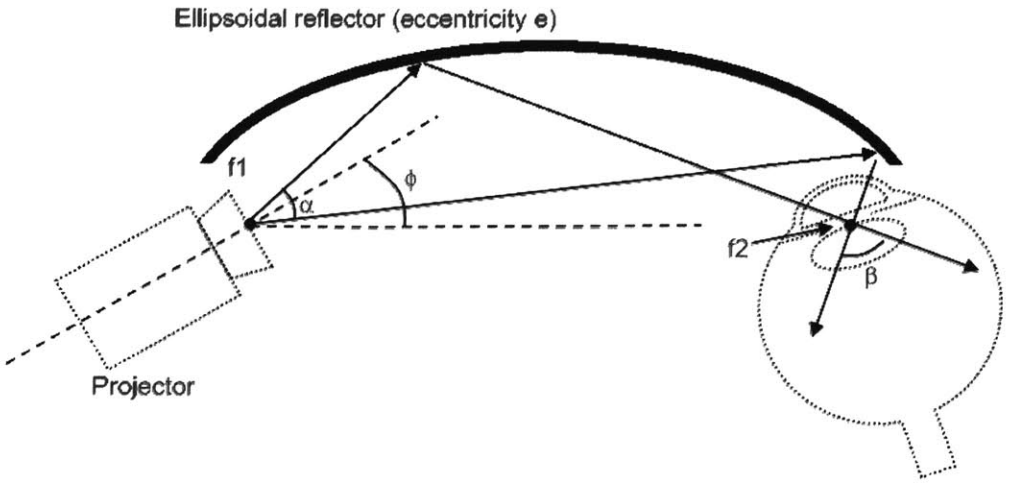

Figure 5-1: Proposed optical design with ellipsoidal reflector for light steering. The pico projector is placed at one focus, f_1 and the eye at the other, f_2. The angle of divergence of light from the projector, α, is fixed, but β can be varied by varying e and ϕ. In this manner the input angle at f_1 can be amplified at f_2.

- Chromatic aberration as the light travels through the lenses
- The maximum sweep angle attainable is constrained by the type of lens used. A lens with a high refractive index would allow a higher sweep angle, but would induce more chromatic aberration, while one of a lower refractive index would induce lower chromatic aberration, but would limit the sweep angle attainable. Combination lenses, such as achromatic lenses, could be used to greatly reduce the chromatic aberration, but this puts practical constraints on the angular sweep to about 40^o.

The concept proposed here draws from advances in optical scanners, specifically those used in Terahertz (THz) imaging applications. Optical scanners are used to mechanically steer beams using movable mirrors and lenses. They are able to achieve image rates of up to a few frames per second (fps) [37]. A common type of optical scanner comprises a pair of galvanometer mirrors that can steer the beam in the horizontal and vertical directions. The apertures (15 to 20 mm) and deflection angles (15 to

20 degrees) necessary to steer beams in the THz part of the spectrum and beyond impose a limitation on achieving frame rates higher than a few fps. Large deflection angles and apertures reduce the speed in which galvanometers can operate to less under 100 Hz, which becomes a significant barrier to imaging in this range.

One of the techniques used to amplify the effect of the moving galvanometers is to place them at the foci of an ellipse. [38]-[41]. The geometric properties of the ellipse then make it possible to vary the amplification factor of the rotation of the galvanometers by varying the eccentricity of the ellipse.

5-1 describes the proposed design [44]. The geometric properties of the ellipse ensure that all the light emitted from focal point f_1 converges at f_2. Thus, if the pico projector used in Chapter 4 is placed at one focal point and the eye at the other, all light emitted by the projector must converge onto the eye. The angle of convergence is a function of the angle of divergence of light emitted by the projector (α), eccentricity (e) of the ellipsoid used and the angle of projection with respect to the major axis of the ellipse, (ϕ). Placing the projector at f_1 and the eye at f_2, as shown in 5-1, would result in the light sheet rotating about the virtual point f_2, which lies within the eye, as desired for capturing cross-sectional images of the anterior segment and the angular sweep range of this light sheet could be varied by varying geometric parameters of the ellipsoid.

5.2 Model

As mentioned earlier, the sweep angle angle of the light sheet at the eye (β) is a function of the angular range of the projector (α), the orientation of the projector with respect to the major axis of the ellipse (ϕ) and the eccentricity of the ellipse (e).

Thus,

$$\beta = g(\alpha, \phi, e) \tag{5.1}$$

The input sweep angle (α) is fixed for a given projector, determined by the internal hardware of the device. Thus, the largest sweep angle achievable (β_{max}) is as follows

$$\beta_{max} = max[g(\phi, e|\alpha)] \tag{5.2}$$

If a ray of light originates from f_1 at an angle ϕ_1 with respect to the major axis of the ellipse and, after reflection, passes through f_2 at an angle of ϕ_2 with respect to the major axis, then, based on the geometric properties of the ellipse,

$$\phi_2(\phi_1) = \pi - [\phi_1 + \arcsin(\frac{2e(1 - e\cos\phi_1)\sin\phi_1}{1 + e^2 - 2e\cos\phi_1})] \tag{5.3}$$

Thus, for a pico projector of angular range α placed at f_1 projecting at an angle of ϕ,

$$\beta = \phi_2(\phi + \alpha/2) - \phi_2(\phi - \alpha/2) \tag{5.4}$$

Reflection by the ellipsoid would cause the input at f_1 to be multiplied by a deterministic factor at f_2. This can be calculated as follows -

$$Multiuplication factor = \frac{\phi_2(\phi + \alpha/2) - \phi_2(\phi - \alpha/2)}{\alpha} \tag{5.5}$$

5-2 suggests that for the highest possible multiplication of input the pico projector **should** be placed such that its projection is centered on the major axis of the ellipse.

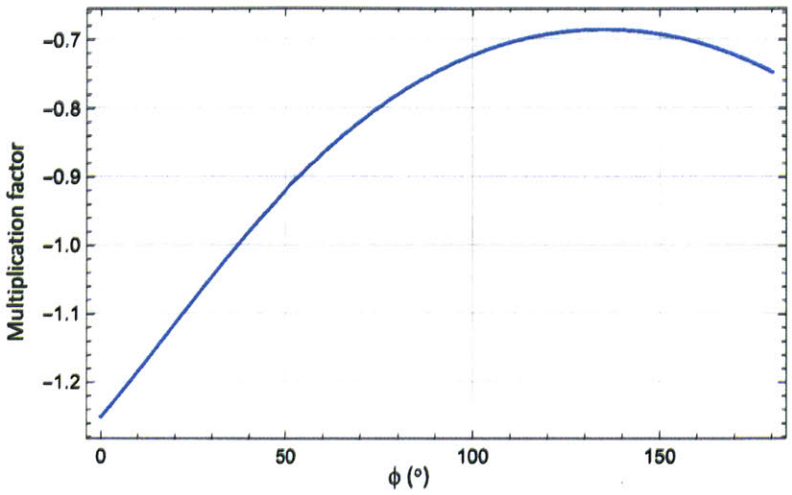

Figure 5-2: Multiplication factor as a function of angle of projection (ϕ) at small α ($\alpha \rightarrow 0$). The highest amplification factor is achieved in the limiting case of $\phi \rightarrow 0$.

Practically, however, placing the pico projector in this manner would result in direct projection onto the eye placed at f_2, without any reflection by the mirrored surface of the ellipsoid.

5-3 shows this same data for a more practical scenario, for an input angle (α) of 10^o and ellipsoid of eccentricity 0.63.

5.3 Path Folding

One of the primary drawbacks of a model such as the one described in 5-1 is the need to place the projector and the eye relatively far apart at different foci. In experiments run with an Edmund Optics 128 mm diameter, 288 mm focal length ellipsoidal reflector this distance worked out to be 27 cm. This results in a fairly large device. Using ellipsoids with similar eccentricities but smaller major axes reduces the tolerance for error in placement of the eye.

To reduce the form factor of the setup while still allowing sufficient tolerance in

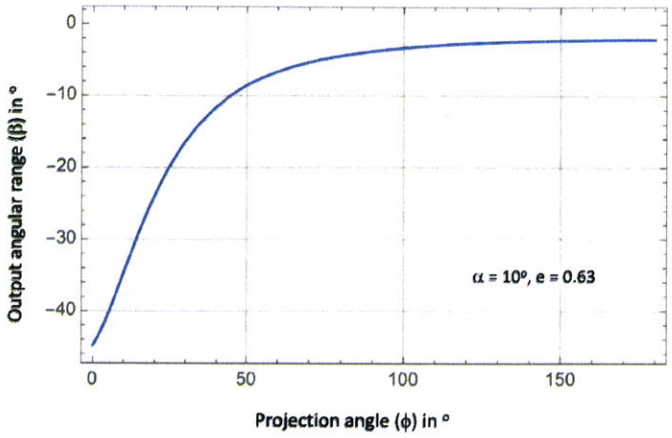

Figure 5-3: Multiplication factor as a function of angle of projection (ϕ) at $\alpha = 10^o$ and eccentricity of ellipsoid (e) = 0.63. This figure represents a more realistic system than that described in figure 5-2. Placing the projector at an angle of about 10^o results in an amplification factor of about 4.

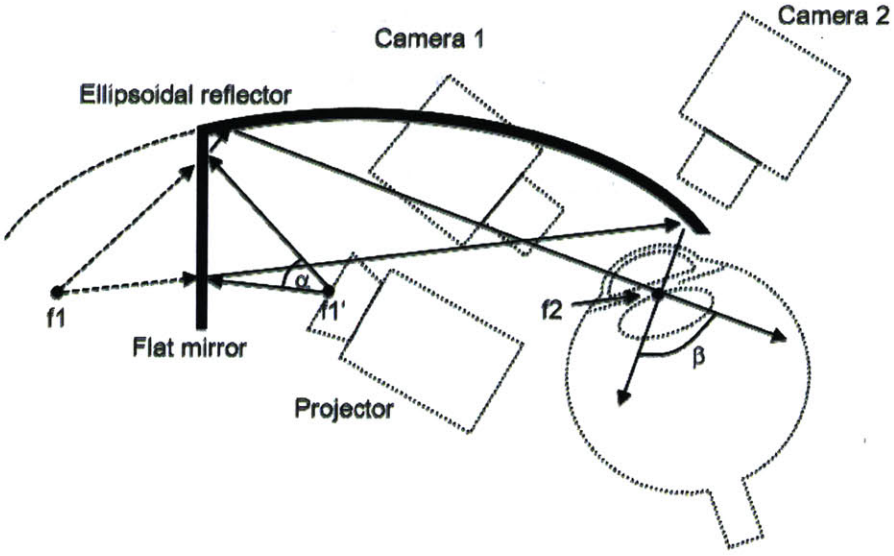

Figure 5-4: Path folding can be used to reduce the form factor of the device. The projector is placed at point f_1', such that the virtual image of the projector in the flat mirror is at the focus f_1 of the ellipsoid. This path folding approach can be repeated infinitely as long as the virtual image of the projector remains at f_1.

placement of the eye, we propose a path folding approach, like that shown in 5-4. In 5-4 the projector is placed at f_1', such that the virtual image of the projector in the flat mirror is at f_1, one of the foci of the ellipse. In this respect, even though the projector is not actually placed at f_1, the light from the projector appears to be emitted from f_1, resulting in it converging onto the eye placed at the other focus, f_2, just as in 5-1. By folding the path of light the effective form factor of the device has been reduced. This path folding approach can be infinitely repeated as long as the virtual image of the projector is eventually at f_1.

5.4 Discussion

The ellipsoidal reflector-based optical design presented in 5-1 allows for multiplication of the input angular range (determined by the properties of the pico projector) by about 4 under ideal conditions (5-3). The theory developed in this chapter helps determine the limits on performance of a programmable illumination-based anterior segment imaging device. This ellipsoidal reflector-based design can be used to build high-end devices for specialized ophthalmic clinics and large hospitals. The designs presented in Chapter 4, however, are most suitable, from a practical standpoint, for development into a device for resource constrained settings.

Chapter 6

Analysis of Deployment Strategies and Impact

6.1 Social Need

With soaring demand for health care, easy accessible solutions for simple and fast health screenings and disease monitoring are sought after [59]. This concept holds true especially for early detection of cataracts, corneal opacities, and pterygia to avert vision loss. Though simple in concept, the hardware complexity of current standard devices (slit lamps) limits their use to specialized ophthalmic clinics and to use by trained professionals, rendering them impractical for resource-constrained settings such as primary care and rural areas. Recent advances in mobile computing, portable imaging, and wireless communication have the potential to enable specialized anterior segment ophthalmic imaging in a point-of-care or even out-of-clinic setting at large scale; this provides new data-driven opportunities for disease detection, diagnosis and treatment.

A WHO study [32] found that in 2002 over 160 million people globally were clinically blind from conditions outside of refractive errors. Almost 60% of these were due to conditions associated with the anterior segment and eyelids, with cataracts alone accounting for 76 million cases. Most conditions of the anterior segment are completely treatable at an early stage, with low to almost no lasting effects on vision. According to another finding of this study, 90% of the worlds visually impaired live in emerging markets. This high prevalence of anterior segment-related blindness is largely arising from poor access to specialized ophthalmic clinics and large hospitals that are taken for granted in major cities and in the developed world. In addition to direct costs associated with diagnosis and treatment, blindness almost always leads to loss of productivity. Even in the United States the total economic burden of vision loss and eye-related disorders is over a $100 billion [33].

The goal of this thesis goal is to radically improve access to eye screenings. The ophthalmic imaging devices presented comprise a smartphone attachment capable of capturing slit lamp-like images of the anterior segment with no additional electronics over what is commonly found in commercial smartphones and a fully automatic programmable illumination-based device that requires little to no operator input, making it ideal for use by untrained nurses for large-scale screening in rural camps and primary care. Post-screening, patients, suspected of having a condition that requires treatment, can be connected with ophthalmologists in larger cities. Improving the screening efficiency will lead to a funnel system for referrals to specialist clinics and dramatically increase the likelihood of a condition being diagnosed early when treatment is most effective.

6.2 Customer Segments

There are three major customer segments this work would benefit [46], as shown in 6-1.

6.2.1 Resource Constrained Settings and Primary Care

The primary application of this thesis would be in resource-constrained settings. This includes rural clinics, war zones, mass screening camps and mobile ophthalmology vans. Current anterior segment imaging technology requires the presence of a trained operator and a specialized ophthalmologist to make inferences from the data. This work focuses on making portable devices that are easy to use and require minimum operator input.

Such devices could be used by untrained nurses for large-scale screening in rural camps and primary care. Patients who are suspected of having conditions requiring treatment can be connected with ophthalmologists in larger cities. This reduces the number of times a patient would need to visit specialized clinics by increasing screening efficiency and increases the likelihood of a condition being diagnosed early.

As stated earlier, in 2002, over 160 million people globally were clinically blind from conditions outside of refractive errors, and 90% of the worlds visually impaired live in developing countries [32]. This is truly a huge unmet need, arising from poor access to specialized ophthalmic clinics and large hospitals that are taken for granted in major cities and the developing world. In addition to direct costs associated with diagnosis and treatment, blindness almost always leads to loss of productivity. Even in a developed country like the United States the total economic burden of vision loss and eye-related disorders is of the order of a $100 billion [33].

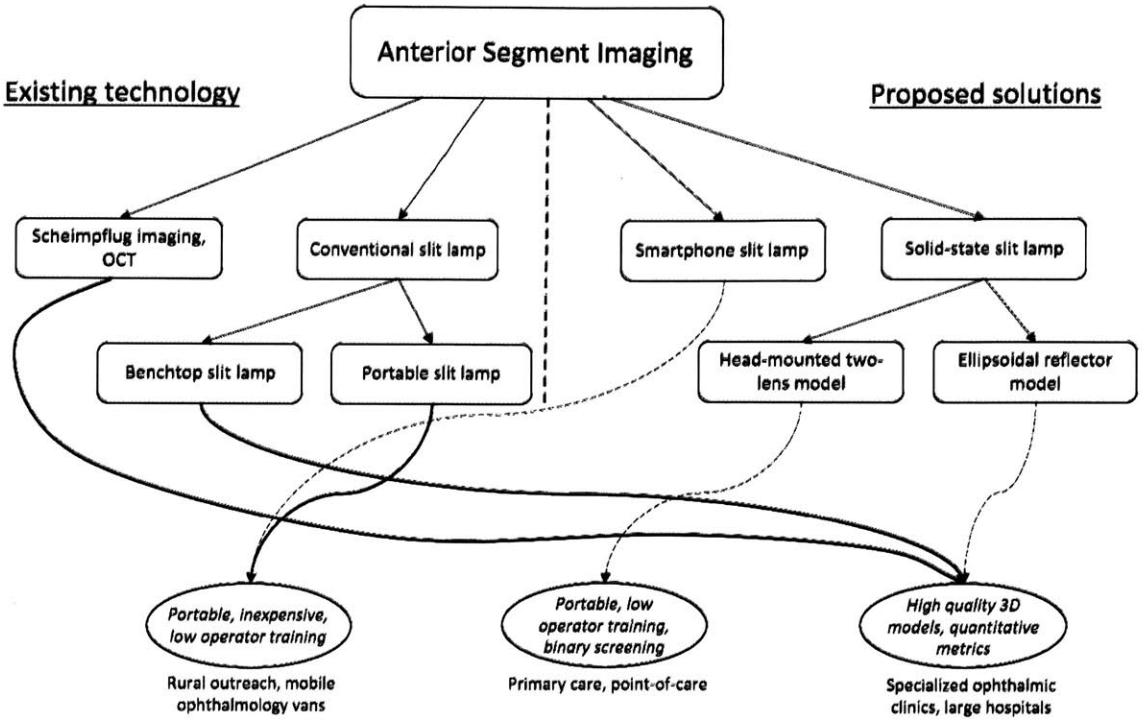

Figure 6-1: Breakdown of existing technology and proposed solutions by use case.

There has also been recent interest in the need for eye exams and other specialist exams at the primary care level [55] [60]-[68] [70] [79] [81]. Most general practitioners learn little ophthalmology, which means it is routine to perform no routine eye exams at the primary care level, and even basic screening for eye conditions must be performed by specialized ophthalmic clinics. Regions lacking specialized ophthalmic clinics Methods have been suggested from increasing the role of optometrists [57] [58] to forming of "community ophthalmic teams" [56] to address this issue. 6-1 helps puts this in perspective.

6.2.2 Specialized Ophthalmic Clinics

A possible secondary application of the programmable illumination-based designs discussed in chapters 4 and 5 would be in existing ophthalmology clinics. Complete

computational control over illumination and a feedback loop between the imaging and illumination modules could, potentially, allow generation of complete 3D models of the anterior segment of the eye that could be used to provide visualization aids and quantitative metrics for easy diagnosis. This capability would make the device preferable to a conventional slit lamp in a specialized ophthalmic clinic or a large hospital in both developing and developed countries.

In a more developed clinic, in addition to slit lamps, more modern imaging modalities like Schiempflug imaging [35] and anterior segment OCT [36] already exist as specialized anterior segment examination tools. The technical limitations in the way these systems are designed make them far more expensive to manufacture than the programmable illumination-based designs discussed earlier. With software post-processing, reconstruction and rendering of the data that is generated by the ellipsoidal reflector based model, it could be possible to generate Pentacam-like data for a fraction of the cost. Specialized ophthalmology, today, is huge market. Over the past decade the market for ophthalmic OCT systems has grown tremendously and was over $300M/year in 2012 [34]. There are now 14 companies making ophthalmic OCT instruments.

6.3 Scalability

We explored the significance of our approach in India during health tech workshops in Mumbai as well as workshops focused on eye diagnostics held at the LV Prasad Eye Institute in Hyderabad, and showed overlap in interest with health care professionals in India. In India, a two-tier hospital system prevails, a) large hospitals with outreach clinics and b) cities without outreach clinics, which would be influenced in distinct ways. Our device will empower less trained employees in the first system, (point-of-care setting), whereas in the latter we will be providing the required hardware as well

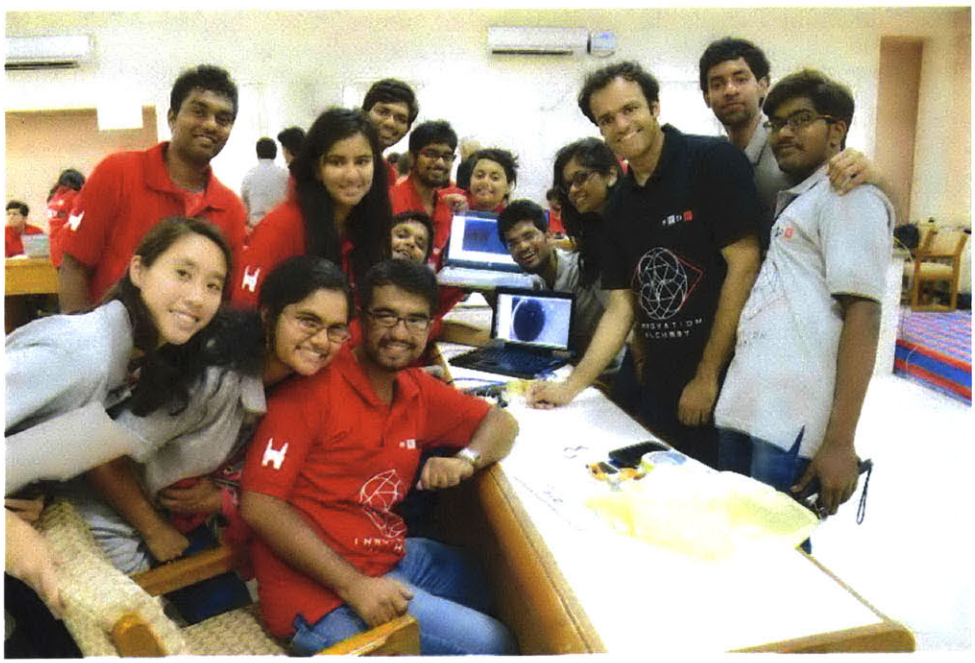

Figure 6-2: The team that worked with engineers from MIT and clinicians from LV Prasad Eye Institute to build programmable illumination-based anterior segment imaging devices during a week-long camp in Hyderabad, India. A subset of this team continued development of these devices in the form of a full-time internship at the LVP-MITRA innovation center. *(Photo: John Werner)*

Figure 6-3: Prototype hardware for the two lens model built in Mumbai during a week-long camp in January 2015 to develop clinic-ready devices specific to the Indian context. Six local innovators worked with MIT engineers and clinicians from the Boston area and India to define the need for portable anterior segment imaging devices in the Indian context. *(Photo: John Werner)*

as the basic required training necessary to operate the devices to health care workers in an outside-clinic setting. Training will include collection of data, transfer of data to telemedicine centers, receiving data from these centers and conveying information back to the patient.

We have established partnerships for initial testing with multiple Indian eye clinics (Aravind in Pondicherry; LVPEI in Hyderabad), which may also be first up-take partners. We have identified specific implementations of this technology suitable for the contrasting cases of LV Prasads structured multi-tier ophthalmic screening network, based out of Hyderabad, and the relatively unstructured healthcare ecosystem prevalent in many tier 2 and tier 3 Indian cities, based out of the city of Nashik in Maharashtra [80].

In the US, improved at-home monitoring and telemedicine could provide a platform to strengthen our technology. We could potentially form a business model similar to that of eyeNETRA [48][50] [78], which operates on a Uber-like service model. We have filed a patent with the US Patent Office (patent pending) [42]. By involving clinical partners in the United States and India, technology licensing and industry liaison personnel at MIT, we feel that we have the initial ingredients for successful and scalable devices that have the potential to create significant impact.

Chapter 7

Conclusion and Future Work

A host of disorders, such as cataracts, corneal opacities, ulcers, pterygia, angle-closure glaucomas etc. affect the anterior segment of the eye and can lead to blindness if left undiagnosed. Specific meaningful clinical interventions are available for each of these common pathologies, but over 160 million people globally are clinically blind [32], primarily sue to poor access to eyecare. The aim of this thesis was to present a range of imaging modalities to image the anterior segment of the eye that are portable and require minimum operator training.

7.1 Summary

In Chapter 3 we presented a 3D printable attachment that fits onto commercial smartphones and is able to redirect the light from the LED flash module to produce slit lamp-like images with no additional electronics. Additionally, we showed how this device could be potentially used in a resource constrained setting and briefly discussed possible deployment strategies.

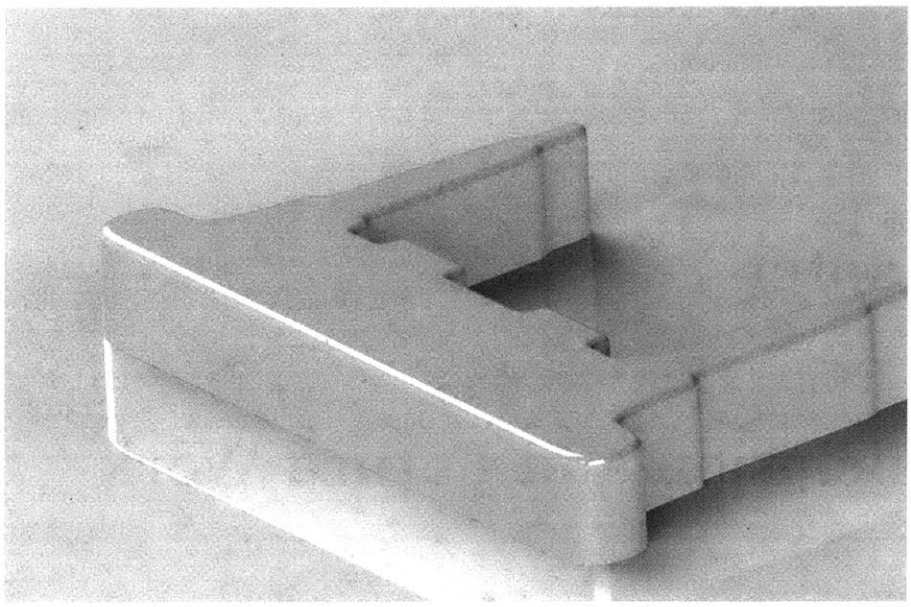

Figure 7-1: Future work: building a portable head-mounted device based on the two lens model, as discussed in 4.5

In Chapter 4 we presented a new modailty to image the anterior segment, using a pico projector to produce a laser light sheet similar to that employed in light sheet fluorescence microscopy. We also showed how this could be built into a benchtop setup and tested our prototype on bovine, porcine and rabbit eyes *ex vivo*. Our programmable illumination-based setup was able to capture high quality cross-sectional views of the animal eyes and we showed how these views change if we mechanically damage the eyes.

In Chapter 5 we presented a different optical design for pico projector-based imaging of the anterior segment, drawing from optical scanners used in THz imaging. We mathematically computed the upper bounds on such a design and presented ways to compress the form factor in order to build a portable device.

Finally, in Chapter 6 we discussed possible customer segments for these devices and analyzed how they could be deployed into different healthcare setups in resource constrained parts of India, as well as business models that could be employed in the

US market.

7.2 Future Work

Future work would primarily involve product development and refinement of the designs presented in this thesis. The head-mounted concept prototype presented in section 4.5 and the smartphone prototype presented in section 3.3 are the closest to conducting research studies on human subjects and actual deployment. The ellipsoidal reflector-based design presented in Chapter 5 would need significant more refinement to reach the stage of being a clinic-ready device, but can serve as a research prototype to design software routines to generate Pentacam-like 3D models of the anterior segment to aid in disease diagnosis.

Bibliography

[1] Barbara Cassin, Sheila A.B. Solomon and Melvin L. Rubin. Dictionary of Eye Terminology. *Triad Publishing Company*, Gainesville, Florida, 1990.

[2] Carl Zeiss Meditec, AG. Eye Examination with the Slit Lamp. Accessed: April 7, 2016.

[3] PFrankoZeitz. Spaltlampenuntersuchung (*translated to English*, Slit Lamp Examination). Accessed May 5, 2016.

[4] Based on Eyesection.gif, by Sathiyam2k. Vectorization and some modifications by ZStardust. Section view of the human eye. Accessed May 5, 2016.

[5] D. M. Maurice. The Structure and Transparency of the Cornea *The Journal of Physiology*, 136(2):263-286, April 1957.

[6] Theodor Scheimpflug. Improved Method and Apparatus for the Systematic Alteration or Distortion of Plane Pictures and Images by Means of Lenses and Mirrors for Photography and for other purposes. *GB Patent No. 1196.* Filed 16 January 1904, and issued 12 May 1904.

[7] David Lieberman, Jonathan Grierson. Method for improving vision. *U.S. Patent No. 6,599,285.* Filed 28 September 2007, and issued 10 April 2008.

[8] A. F. Fercher, K. Mengedoht and W. Werner. Eye-length measurement by interferometry with partially coherent light. *Optics Letters.* 13(3):186-188. 1988.

[9] J. M. Schmitt. Optical coherence tomography (OCT): a review. *IEEE Journal of Selected Topics in Quantum Electronics.* 5(4):1205-1215. 1999.

[10] J. P. Ganley and J. Roberts. Eye conditions and related need for medical care. *Vital and health statistics.* 11(228):1-69. 1982.

[11] Eilhard Koppenhfer. From Lateral Illumination to the Slit Lamp - A Brief Outline of Medical History. Accessed April 7, 2016

[12] Haag Streit Diagnostics (May 6th, 2016) BA 904 Retrieved from http://www.haag-streit.com/haag-streit-diagnostics/products/slit-lamps/ba-904/

[13] Keeler Ophthalmic Instruments (May 6th, 2016) Keeler PSL Portable Slit Lamps Retrieved from http://www.keelerusa.com/ophthalmic/index.php/products/slit-lamps/portable-slit-lamps.html

[14] Reichert Technologies (May 6th, 2016) Reichert Portable Slit Lamps Accessed May 6, 2016

[15] Topcon Medical Systems, Inc. (May 6th, 2016) Topcon SL-D7 Retrieved from http://www.topconmedical.com/products/sld7.htm

[16] HEI Laboratories, Inc. (May 6th, 2016) Digital Video Slit Lamps Retrieved from http://hailabs.com/products/slit-lamp/

[17] Keeler Keeler 40H Digital Slit Lamp Retrieved from http://www.keelerusa.com/ophthalmic/index.php/products/slit-lamps/40h-slit-lamps.html

[18] Wendy W. Lee Slit Lamp Adapters turn Smartphones into Clinical Cameras *Ophthalmology Web.* 2013.

[19] Jan Bond Chan, Hao Chi Ho, Nor Fariza Ngah and Elias Hussein DIY Smartphone Slit-Lamp adaptor *Journal of Mobile Technology in Medicine.* 3:1:1622. 2014.

[20] Tiger Lens Tiger Lens - turn your iPhone into a slitlamp digital imaging system Accessed May 6, 2016

[21] OCULUS OCULUS Pentacam Retrieved from http://www.pentacam.com/sites/index.php

[22] J. A. Izatt, M. R. Hee, E. A. Swanson, C. P. Lin, D. Huang, J. S. Schuman, C. A. Puliafito and J. G. Fujimoto. Micrometer-scale resolution imaging of the anterior eye in vivo with optical coherence tomography. *Archives of Ophthalmology.* 112(12):1584-9. 1994.

[23] S. Radhakrishnan, A. M. Rollins, J. E. Roth, S. Yazdanfar, V. Westphal, D. S. Bardenstein and J. A. Izatt Real-time optical coherence tomography of the anterior segment at 1310 nm. *Archives of Ophthalmology.* 119(8):1179-85. 2001.

[24] S. Fukuda, K. Kawana, Y. Yasuno and T. Oshika. Repeatability and reproducibility of anterior ocular biometric measurements with 2-dimensional and 3-dimensional optical coherence tomography. *Journal of Cataract and Refractive Surgery.* 36(11):1867-73. 2010.

[25] Sanjay Asrani, Marinko Sarunic, Cecilia Santiago and Joseph Izatt. Detailed Visualization of the Anterior Segment Using Fourier-Domain Optical Coherence Tomography. *Archives of Ophthalmology.* 126(6): 765771. 2008.

[26] Vaibhav Vaish, Bennett Wilburn, Neel Joshi and Marc Levoy. Using Plane + Parallax for Calibrating Dense Camera Arrays. *Proceedings of the IEEE Conference on Computer Vision and Pattern Recognition (CVPR).* 2004.

[27] J. B. Pawley. Handbook of Biological Confocal Microscopy (3rd edition). *Springer.* 2006.

[28] K. Greger, J. Swoger and E. H. Stelzer. Basic building units and properties of a fluorescence single plane illumination microscope. *The Review of Scientific Instruments.* 78(2):023705. 2007.

[29] T. Rabsilber, R. Khoramnia and G. Auffarth. Anterior chamber measurements using Pentacam rotating Scheimpflug camera. *Journal of Cataract and Refractive Surgery.* 32(3):456-9. 2006.

[30] P. Berard, D. Bradley, M. Nitti, T. Beeler and M. Gross. *ACM Transactions on Graphics (TOG) - Proceedings of ACM SIGGRAPH Asia.* 33(6):223:1-12. 2014.

[31] K. Ruhland, S. Andrist, J. Balder, C. Peters, N. Badler, M. Gleicher, B. Mutlu and R. McDonnell. Look me in the eyes: A survey of eye and gaze animation for virtual agents and artificial systems. *Eurographics State of the Art Reports.* p69-91. 2014.

[32] World Health Organization and the International Agency for the Prevention of Blindness. Vision 2020: The Right to Sight. Accessed October 5, 2015.

[33] J.S. Wittenborn and D.B. Rein. Cost of Vision Problems: The Economic Burden of Vision Loss and Eye Disorders in the United States, 2013 Accessed October 5, 2015.

[34] Optical Coherence Tomography News. Estimates of Ophthalmic OCT Market Size and the Dramatic Reduction in Reimbursement Payments. Accessed October 5, 2015.

[35] Rajeev Jain. Pentacam: Principle and Clinical Applications. *Journal of Current Glaucoma Practice.* 3(2):20-32. 2009.

[36] Alissa Coyne and Joseph Shovlin. AS-OCT Technology: Analyzing the Anterior Segment. *Review of Optometry.* 2012.

[37] Q. Song, Y. Zhao, A. Redo-Sanchez, C. Zhang, and X. Liu. Fast continuous terahertz wave imaging system for security *Optics Communication.* 282(10):2019-2022. 2009.

[38] Antonio Garca-Pino, Nuria Llombart, Borja Gonzalez-Valdes, and Oscar Rubios-Lpez. A Bifoca lEllipsoidal Gregorian Reector System for THz Imaging Applications. *IEEE Transactions on Antennas and Propogation.* 60(9):4119-28. 2012.

[39] Nuria Llombart, Ken B. Cooper, Robert J. Dengler, Tomas Bryllert, and Peter H. Siegel. Confocal Ellipsoidal Reector System for a Mechanically Scanned Active Terahertz Imager. *IEEE Transactions on Antennas and Propogation.* 58(6):1834-41. 2010.

[40] Ken B. Cooper, Robert J. Dengler, Nuria Llombart, Ashit Talukder, Anand V. Panangadan, Chris S. Peay, Imran Mehdi, Peter H. Siegel. Fast, high-resolution terahertz radar imaging at 25 meters. *SPIE Proceedings on Terahertz Physics, Devices, and Systems IV: Advanced Applications in Industry and Defense.* 76710Y-1-8. 2010.

[41] Alexander V. Belinsky and Alexander V. Plokhov. High-speed Framing Camera with an Ellipsoidal Scanner. *OSA Applied Optics.* 34(1):174-176. 1995.

[42] Shantanu Sinha, Albert Redo-Sanchez, Vincent James Patalano II, Pushyami Rachapudi, Nickolaos Savidis, Everett Lawson, Hyunsung Park, Ramesh Raskar. Methods and Apparatus for Anterior Segment Oculus Imaging. *U.S. Patent No. 15,000,032.* Filed January 2016. Patent Pending.

[43] S. Sinha, N. Savidis, E. Lawson, R. Raskar. Replacing the Slit Lamp with a Mobile Multi-Output Projector Device for Anterior Segment Imaging. *Association for Research in Vision and Ophthalmology Annual Meeting.* 2015.

[44] P. Rachapudi, S. Sinha, W. Lee, A. Redo-Sanchez, R. Raskar. A purely solid-state device for rapid reconstruction of 3D models of the anterior segment of the eye with no moving parts. *Association for Research in Vision and Ophthalmology Annual Meeting.* 2016.

[45] S. Sinha, W. Lee, R. Raskar. A Smartphone attachment for slit lamp-like imaging of the anterior segment of the eye. *Association for Research in Vision and Ophthalmology Annual Meeting.* 2016.

[46] Cheryl Guttman Krader. Low-cost mobile alternative to the slit lamp brings the benefits of greater convenience and broader utility. *EuroTimes Stories.* September issue. 2015.

[47] K. C. Richardson. The fine structure of the albino rabbit iris with special reference to the identification of adrenergic and cholinergic nerves and nerve endings in its intrinsic muscles. *American Journal of Anatomy* 114(2):173-205. 1964.

[48] EyeNetra EyeNetra - Smartphone-powered Refraction. Retrieved from https://eyenetra.com/

[49] T. Swedish, K. Roesch, I.K. Lee, K. Rastogi, S. Bernstein and R. Raskar. eyeSelfie: Self Directed Eye Alignment using Reciprocal Eye Box Imaging. *ACM Transactions on Graphics - Proc. of SIGGRAPH 2015* 34(4):58:1-10. 2015.

[50] V. F. Pamplona, A. Mohan, M. M. Oliveira and R. Raskar. NETRA: Interactive Display for Estimating Refractive Errors and Focal Range. *ACM Transactions on Graphics - Proceedings of SIGGRAPH* 29(4):77:1-8. 2010.

[51] V. Pamplona, E. Passos, J. Zizka, M. Oliveira, E. Lawson, E. Clua and R. Raskar. CATRA: Cataract Probe with a Lightfield Display and a Snap-on Eyepiece for Mobile Phones. *ACM Transactions on Graphics - Proceedings of SIGGRAPH.* 30(4):47:1-8. 2011.

[52] F.C. Huang, G. Wetzstein, B. Barsky and R. Raskar. Eyeglasses-free Display: Towards Correcting Visual Aberrations with Computational Light Field Displays. *ACM Transactions on Graphics - Proceedings of SIGGRAPH.* 33(4):59:1-12. 2014.

[53] A. Maimone, G. Wetzstein, D. Lanman, M. Hirsch, R. Raskar and H. Fuchs. Focus 3D: Compressive Accommodation Display. *ACM Transactions on Graphics.* 32(5):153:1-13. 2013.

[54] D. Lanman, G. Wetzstein, M. Hirsch, W. Heidrich and R. Raskar. Beyond Parallax Barriers: Applying Formal Optimization Methods to Multi-Layer Automultiscopic Displays. *SPIE Stereoscopic Displays and Applications XXIII* 82880A 10.1117/12.907146. 2012.

[55] R. Smith. Primary care ophthalmology. *British Journal of Ophthalmology.* 90(6):669-670. 2006.

[56] R. K. Blach. The delivery of ophthalmic care: the practitioner, community ophthalmic teams and contract ophthalmology. *British Journal of Ophthalmology.* 85:12745. 2001.

[57] S. Dorrell. Primary care: the future. *London: Department of Health.* 1996.

[58] A. Ewbank. The optometrist and primary eye care. *British Journal of Ophthalmology.* 81(2):1001. 1997.

[59] R. Raskar. How do we look at the future of health with both eyes? *TEDMED 2013.* Washington D. C. 2013.

[60] A. J. Das, T. A. Valdez, J. A. Vargas, P. Saksupapchon, P. Rachapudi, Z. Ge, J. C. Estrada, and R. Raskar. Volume estimation of tonsil phantoms using an oral camera with 3D imaging. *Biomedical Optics Express.* 7:1445-1457. 2016.

[61] A. J. Das, J. C. Estrada, Z. Ge, S. Dolcetti, D. Chen and R. Raskar. A compact structured light based otoscope for three dimensional imaging of the tympanic

membrane. *Proceedings of SPIE 9303, Photonic Therapeutics and Diagnostics XI.* 93031F. 2015.

[62] G. Leifman, T. Swedish, K. Roesch and R. Raskar. Leveraging the Crowd for Annotation of Retinal Images. *International Conference of the IEEE Engineering in Medicine and Biology Society.* 2015.

[63] G. Satat, D. Raviv, B. Heshmat and R. Raskar. Imaging through thick turbid medium using time-resolved measurement. *Computational Optical Sensing and Imaging.* CT3F. 4. 2015.

[64] G. Satat, B. Heshmat, C. Barsi, D. Raviv, O. Chen, M. G. Bawendi and R. Raskar. Locating and classifying fluorescent tags behind turbid layers using time-resolved inversion. *Nature Communications* 6:6796. doi: 10.1038/ncomms7796. 2015.

[65] G. Satat, C. Barsi and R. Raskar. Skin Perfusion Photography. *IEEE Conference on Computational Photography.* 2014.

[66] N. Naik, C. Barsi, A. Velten and R. Raskar. Time-resolved reconstruction of scene reflectance hidden by a diffuser. *CLEO: Science and Innovations.* CTu1H. 2013.

[67] A. Kadambi, H. Ikoma, X. lin, G. Wetzstein and R. Raskar. Subsurface enhancement through sparse representations of multispectral direct/global decomposition. *Computational Optical Sensing and Imaging* CTh1B. 2013.

[68] C. Barsi, A. Velten, M. Lorrainy-Altoe, A. Rehman and R. Raskar. Spectral encoding enhances visual flexibility of surgical endoscopes. *SPIE Biomedical Optics Conference.* 89351E-89351E-6. 2013.

[69] G. Wetzstein, D. Lanman, M. Hirsch and R. Raskar. Real-time Image Generation for Compressive Light Field Displays. *Journal of Physics: Conference Series.* 415 (1), 012045. 2013.

[70] C. Barsi, R. Whyte, A. Bhandari, A. Das, A. Kadambi, A. A. Dorrington and R. Raskar. Multi-frequency reference-free fluorescence lifetime imaging using a time-of-flight camera. *OSA Biomedical Optics.* BM3A. 2014.

[71] D. Wu, G. Wetzstein, C. Barsi, T. Willwacher, Q. Dai and R. Raskar. Ultra-fast Lensless Computational Imaging through 5D Frequency Analysis of Time-resolved Light Transport. *nternational Journal of Computer Vision.* 110(2):128-140. 2014.

[72] B. masia, G. Wetzstein, C. Aliaga, R. Raskar and D. Gutierrez. Display adaptive 3D content remapping. *Computer and Graphics.* 37(8):983-996. 2013.

[73] D. Lanman, G. Wetzstein, M. Hirsch and R. Raskar. Depth of Field Analysis for Multilayer Automultiscopic Displays. *Journal of Physics: Conference Series.* 415(1), 012036. 2013.

[74] M. Hirsch, D. Lanman, G. Wetzstein and R. Raskar. Construction and Calibration of Optically Efficient LCD-based Multi-Layer Light Field Displays. *Journal of Physics: Conference Series.* 415 (1), 012071. 2013.

[75] F. C. Huang, G. Wetzstein, B. A. Barsky and R. Raskar. Computational light field display for correcting visual aberrations. *ACM SIGGRAPH Posters.* 2013.

[76] L. Hardesty. Vision-correcting Displays. *MIT News.* July 31, 2014.

[77] L. Hardesty. Glasses-free 3-D Projector. *MIT News.* May 16, 2014.

[78] R. Raskar. Eye Netra. *TEDx Gateway..* 2015.

[79] L. Hardesty. Biomedical imaging at one-thousandth the cost. *MIT News.* November 23, 2015.

[80] S. Parikh and B. Miller. Innovating for Billions. *MIT News*. March 9, 2016.

[81] L. Zimmerman. Superhuman Vision. *MIT News*. October 6, 2014.